Advance Sustainable Science, Engineering and Technology (ASSET)
Vol. 8, No.3, July 2026, pp. 02603027-01 ~ 02603027-012
ISSN: 2715-4211 DOI: https://doi.org/10.26877/asset.v8i3.2473

Structural Stability Assessment of a Floating Fiber Composite Levee under Variable Tidal Loading: A Laboratory and Finite Element Approach

Sunaryo [1,2*], Slamet Imam Wahyudi[1], Moh. Faiqun Ni'am[1], Adam Safitri[3]

[1]Civil Engineering Doctoral Program, Faculty of Engineering, Sultan Agung Islamic University, Semarang, Indonesia

[2]Civil Engineering Study Program, Faculty of Engineering, Wiralodra University, Indramayu, Indonesia

[3]Civil Engineering Study Program, Sekolah Tinggi Teknologi Cirebon, Indonesia

*joykusuma50@gmail.com

Abstract. This study investigated the structural stability of a floating fiber composite levee model subjected to hydrostatic loading under three tidal scenarios: 50 cm (Scenario I), 75 cm (Scenario II), and 100 cm (Scenario III). Laboratory experiments were conducted in a glass test tank (70 cm × 17 cm × 6.5 cm), and results were validated using ANSYS Static Structural finite element analysis. Hydrostatic pressure ranged from 4,905 to 9,810 N/m², with maximum stress ranging from 11,207 to 89,656 N/m². Total deformation increased from 7.68×10^{-7} m to 1.23×10^{-5} m across scenarios. Shear safety factors ranged from 8.04 (Scenario I) to 2.01 (Scenario III), and overturning moment safety factors declined from 10.04 to 2.50. Numerical results showed deviation below 1% compared to manual calculations, confirming model reliability. These findings confirm the prototype-scale feasibility of the floating fiber levee concept, though scale-up validation and material reinforcement are required before field implementation.

Keywords: Floating levee, fiber composite, hydrostatic stability, coastal protection, finite element analysis.

(Received 2025-07-31, Revised 2026-04-20, Accepted 2026-07-24, Available Online by 2026-07-31)

1. Introduction

Intensifying climate change has accelerated sea level rise and coastal flooding worldwide. Indonesia, as the world's largest archipelagic nation with over 17,000 islands, is highly vulnerable: more than 2,000 islands are projected at risk of submergence, with coastal areas in Sumatra, Java, and Kalimantan facing direct threats [1]. Specifically, approximately 405,000 hectares of coastal land are projected to be affected by this process, ultimately exacerbating the impacts of tidal flooding [2], [3]. Meanwhile, critical coastal ecosystems such as mangroves and coral reefs—which function as natural protective barriers—have become increasingly threatened by climate change, further increasing vulnerability to flood and erosion risks [4], [5].

Frequent tidal floods have damaged coastal infrastructure such as roads, bridges, and public facilities essential to coastal economies. In addition, the increasing frequency of tidal flooding has also impacted livelihoods, especially for those living in informal settlements that are prone to inundation [6]–[8]. Conventional levees, the typical response to these threats, are static and not sufficiently adaptive to extreme tidal fluctuations driven by climate change [9], [10]. This calls for the development of new solutions that are more flexible, sustainable, and capable of adapting rapidly to rising sea levels.

To address these limitations, this study proposes a floating fiber levee model equipped with an automatic hydraulic system that adjusts levee height in real time according to sea level fluctuations. The fiber composite structure offers greater durability, lightness, and lower maintenance cost than conventional materials such as concrete or earth fill [11], [12].

Existing barriers—static earthen levees, sheet pile walls, and inflatable rubber dams—offer limited adaptability to fluctuating sea levels [9], [10]. Self-closing flood barriers offer automatic actuation but are typically built from rigid materials that add weight and installation cost [19]. Composite fiber materials have been applied in lightweight structural systems with high corrosion resistance [15], [16], yet integration into a dynamically adjusting levee has not been structurally validated for coastal hydrostatic conditions.

However, key concerns remain regarding the stability and durability of the floating fiber material under hydrostatic pressure and larger-scale implementation. This study therefore tested the model's performance through laboratory experiments and evaluated its applicability to Indonesian coastal regions prone to tidal flooding, using ANSYS simulation to replicate physical conditions and predict performance under more extreme conditions [13], [14].

Fiber composite technology, already proven effective in other construction sectors, offers high strength and low weight compared to concrete, reducing transportation and installation costs [15], [16], [17], [18], [19], [20]. Fiber materials are also anti-corrosive, making them well suited to seawater exposure. This study hypothesized that a hydraulically actuated floating fiber levee would adapt more effectively to dynamic sea level changes than static conventional levees.

Most existing studies have addressed fiber composites in lightweight structural applications, but few have directly addressed their implementation in coastal defense systems [21], [22], [23], [24], [25], and no study has combined fiber composites with automatic hydraulic actuation for Indonesia's coastal zones.

The objective of this research was to design, develop, and test a floating fiber levee model based on an automatic hydraulic system, evaluating its effectiveness and resilience under extreme tidal conditions in Indonesia's coastal regions through combined experimental and numerical methods.

Despite growing interest in adaptive coastal infrastructure, no previous study has examined the combined application of hollow fiber composite material and an automatic hydraulic adjustment system in a floating levee configuration assessed through both physical laboratory testing and ANSYS finite element validation. Existing research has addressed fiber composites in structural applications [21]–[25] and self-closing flood barriers [19], but these studies do not evaluate the integrated hydrostatic stability, shear resistance, and overturning moment behavior of a buoyancy-driven levee prototype under multiple tidal scenarios. This study therefore addresses that gap by providing the first laboratory-scale structural stability assessment of a floating fiber composite levee validated against ANSYS Static Structural simulation across three tidal loading conditions.

This research thus contributes to coastal defense technology based on fiber composites and automatic hydraulic systems, offering a practical, adaptive strategy for protecting Indonesian coastal areas from climate change impacts.

2. Methods

This study aimed to develop and analyze a floating fiber levee model equipped with an automatic hydraulic system as a climate change mitigation strategy, particularly in addressing the impacts of sea level rise that can trigger tidal flooding.

The research was conducted using two main approaches: laboratory experiments and numerical simulations using ANSYS software. The laboratory experiments aimed to obtain empirical data regarding the behavior of the floating fiber levee model under various tidal conditions, while the numerical simulations using ANSYS aimed to validate the experimental results and provide deeper insight into the levee structure's response to hydrodynamic pressure.

2.1. Laboratory Experiment

The laboratory experiment was conducted using a scaled model of a floating fiber levee placed in a water-filled test tank. The test tank was constructed from transparent glass materials, with dimensions of 6.5 cm in width, 17 cm in height, and 70 cm in length. The schematic and model of the test tank are illustrated in Figures 3.1 and 3.2.

Inside the test tank, the prototype levee was fabricated using hollow fiber material coated with composite fiber and placed at the base of the tank. The fiber composite material used in this study consisted of a hollow fiber core wrapped with glass fiber-reinforced polymer (GFRP) layers. Based on standard material characterization for GFRP composites used in structural applications, the material properties applied were: elastic modulus of 25 GPa, tensile strength of 350 MPa, density of 1,800 kg/m^3, and Poisson's ratio of 0.25. The levee prototype had an overall wall thickness of 5 mm, a total height of 15 cm, and a base width of 6 cm. The prototype was constructed at a geometric scale ratio of 1:10 relative to a hypothetical full-scale structure, consistent with the dimensional constraints of the laboratory test tank and the objective of observing relative hydrostatic behavior under controlled tidal conditions. The levee model was tested under three tidal scenarios: at ½ of the maximum water height, ¾ of the maximum water height, and full high tide (maximum water height). These scenarios aimed to observe the levee's position, deformation, buoyant force, and pressure under different tidal conditions.

Several instruments were used to support the testing, including a diver sensor to measure the water level in the test tank, and a hydraulic motor system to lift and adjust the levee position in response to rising water levels.

The diver sensor (submersible pressure transducer) had a measurement range of 0 to 200 cm water column with an accuracy of ±2 mm and a resolution of 0.1 mm. The sensor was calibrated prior to each test series using a graduated reference water column under static conditions to ensure measurement consistency across all scenarios. The hydraulic motor system operated at a rated working pressure of 6 bar, with a maximum lifting capacity of 5 kg, which was sufficient to actuate the prototype levee across the full range of tested water heights. All sensor data were recorded at a sampling interval of 1 second using a data logger connected to a laptop computer. Measurement uncertainty for water level readings was estimated at ±1.5%, accounting for sensor drift and minor surface wave disturbances in the test tank. Visual observations supplemented the sensor data to document the levee's hydrodynamic behavior throughout each test.

2.2. Research Variables

The independent variables were levee type and tidal height/frequency; dependent variables were levee position, deformation, buoyant force, and applied pressure; and controlled variables were the fiber material, surface area, and mass of the levee, isolating the influence of each factor and minimizing external disturbances.

2.3. Numerical Simulation

Numerical simulations in ANSYS software modeled the levee under conditions equivalent to the laboratory tests, validating experimental results and providing further insight into performance under more extreme conditions. The simulation process began with geometric modeling in ANSYS Design Modeler, followed by application of boundary conditions—water height and buoyant force—matching the laboratory setup.

The ANSYS Static Structural module (ANSYS Mechanical 2023 R1) was used with a three-dimensional solid element model. The levee geometry was discretized using SOLID186 20-node hexahedral elements, which are well-suited for curved thin-walled composite structures under surface pressure loading. A mesh sensitivity study was performed, and a final maximum element size of 3 mm was selected, yielding approximately 18,500 nodes and 4,200 elements with an average mesh quality skewness of 0.35, well within the acceptable threshold of 0.7. Isotropic linear elastic material properties were assigned to all elements, consistent with the bulk GFRP material characterization described above. Boundary conditions were defined as follows: a fixed support was applied at the levee base to simulate the anchor constraint imposed by the test tank floor, and hydrostatic pressure was applied as a distributed surface load on the upstream face of the levee, calculated using the relation $P = \rho \cdot g \cdot h$ for each tidal scenario, where $\rho = 1{,}000$ kg/m³ and $g = 9.81$ m/s². Solution convergence was verified by monitoring displacement and von Mises stress residuals, with a convergence criterion of 0.1%. The analysis was conducted under static equilibrium assumptions, and dynamic wave effects were not considered in this study, consistent with the quasi-static nature of the laboratory tidal loading protocol.

Simulation outputs—stress distribution, deformation, and translation patterns under each tidal condition—were compared with laboratory outcomes to validate model accuracy and assess consistency between numerical and experimental findings.

2.4. Static Structural Analysis of the Levee

Static structural analysis calculated the normal loads, moments, and torque generated by water pressure, from which ANSYS-derived deformation, displacement, and stress values were used to determine the levee's safety factors and compared against laboratory test data.

2.5. Validation and Comparative Analysis of Experimental and Numerical Results

Results from laboratory experiments and ANSYS simulations were compared to validate differences in deformation, buoyant force, and pressure acting on the levee under experimental and numerical conditions. Agreement between experimental and numerical results was evaluated using percentage deviation (%) calculated as $|(\text{experimental} - \text{simulation}) / \text{experimental}| \times 100\%$, with a target threshold of less than 5% considered acceptable for engineering validation purposes. Key parameters analyzed included maximum levee displacement, peak pressure, and recovery time after disturbance, with discrepancies traced to potential measurement error, friction, or other unmodeled factors.

2.6. Research Workflow

The study proceeded through a literature review, laboratory testing of the floating fiber levee prototype, and numerical simulation using ANSYS, with results from both approaches analyzed to draw the conclusions presented in the following section. The overall research flow is presented in Figure 1.

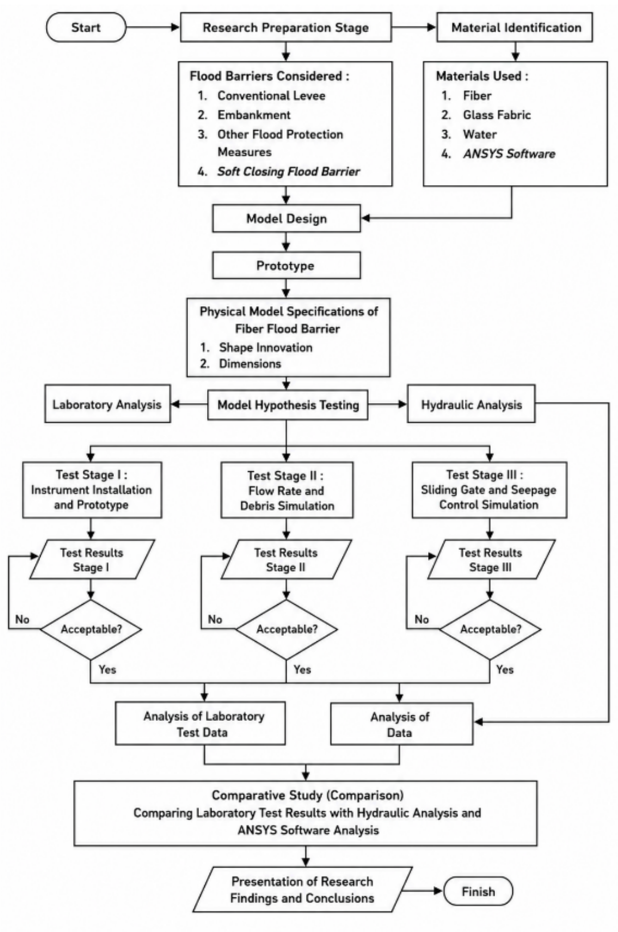

Figure 1. Research Flow Diagram

3. Results and Discussion

This section presents the stability and performance of the floating fiber levee model under three tidal scenarios, based on laboratory experiments and ANSYS simulations, covering hydrostatic pressure, shear, overturning moment, and buoyancy in each case.

3.1. Static Structural Analysis of the Levee

In the first scenario, representing medium tidal conditions (h = 50 cm), the force diagram acting on the prototype floating levee is shown in Figure 2. Based on calculations, the hydrostatic pressure acting on the fiber levee was determined using the hydrostatic pressure formula, as follows:

$$PB1 = \gamma \times h \tag{1}$$

$$\begin{aligned} PB1 &= \gamma \times h \\ &= 9.810 \times 0.5 \\ &= 4.905 \text{ Kg/m.s}^2 \end{aligned}$$

The total hydrostatic force was calculated as:

$$FH1 = PA1 \times A \tag{2}$$

$$\begin{aligned} FH1 &= PA1 \times A \\ &= 4.905 \times 1 \\ &= 4.905 \text{ Kg m/s}^2 \end{aligned}$$

In addition, the moment generated by water pressure was calculated as:

$$M = F \times yc \quad (3)$$

$$M = F \times yc$$
$$= 1.635 \text{ Kg m/s}^2\text{.m}$$

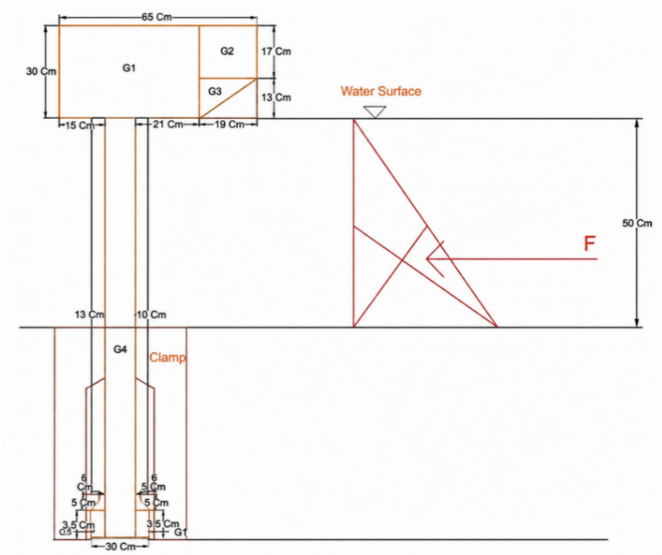

Figure 2. Force Diagram of the Prototype Levee – Scenario I

Based on the calculations conducted in Scenario I, the characteristic values such as hydrostatic pressure, maximum stress, strain, and deformation of the floating fiber levee prototype are presented in Table 1. The table shows that in Scenario I, the hydrostatic pressure on the levee was 4.905 $\text{Kg/m}^2\text{.s}^2$, the maximum stress was 11.206,995 $\text{Kg/m}^2\text{.s}^2$, and the resulting deformation was 7,68 x 10^{-7}m. Shear force reached 2.452,500 Kg m/s^2 , and the safety factor for shear was 8,04, maintaining structural stability. Overturning moment analysis showed a hydrostatic moment of 817,450 Kg/m.s^2 and a resisting moment from the levee weight of 8211,052 Kg/m.s^2 ..m, resulting in a safety factor of 10,04.

Table 1. Summary of Prototype Testing Results – Scenario I | Scenario II | Scenario III

Parameter	**Unit**	**Scenario I**	**Scenario II**	**Scenario III**
Hydrostatic Pressure	$\text{Kg/m}^2\text{.s}^2$	4905,000	7357,500	9810,000
Maximum Stress (σ)	$\text{Kg/m}^2\text{.s}^2$	11206,995	37823,607	89655,956
Strain (ε)	–	1,54 x 10^{-6}	5,18 x 10^{-6}	1,23 x 10^{-5}
Deformation (δ)	m	7,68 x 10^{-7}	3,89 x 10^{-6}	1,23 x 10^{-5}
Safety Factor Of Shear	–	8,04	3,57	2,01
Safety Factor Of Moment	–	10,04	4,49	2,50

3.2. Static Structural Analysis Using ANSYS

In Scenario I, numerical simulation using ANSYS indicated that the maximum hydrostatic pressure at the levee base was 4.905 Kg/m.s^2 (Figure 3a). Stress analysis showed a maximum of 11.196 Kg/m.s^2, strain of 1,44 x 10^{-6} and total deformation was 7,63 x 10^{-7} m (Figure 3b – 3d). These results demonstrated that the fiber levee model remained stable under the given hydrostatic pressure.

Shear force generated by water flow was 2.452,500 Pa or 2.452,500 Kg m/s^2 (Figure 8). The shear stability analysis produced a safety factor (SF) of 8,03, indicating strong resistance to shear failure. Overturning moment analysis showed a hydrostatic moment of 817,450 Nm or 817,450 Kg m/s^2.m and a resisting moment from the levee weight of 8.211,052 Kg m/s^2.m resulting in a safety factor of 10,04 (Figure 3e- Figure 3f).

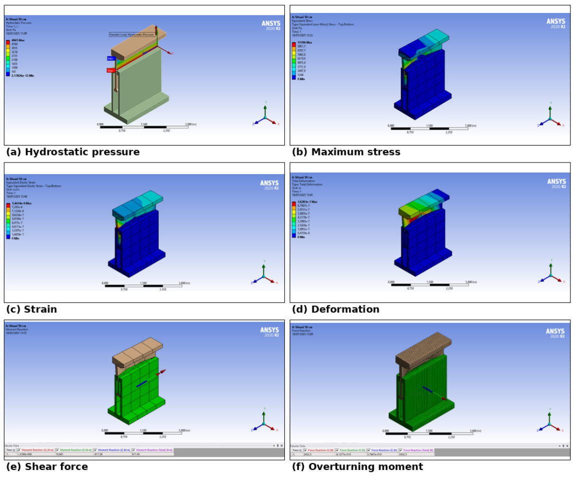

Figure 3. Static structural results for Scenario I (h = 50 cm): (a) hydrostatic pressure, (b) maximum stress, (c) strain, (d) deformation, (e) shear force, (f) overturning moment (ANSYS Static Structural)

Scenario II represented ¾ of peak tidal height (h = 75 cm). Hydrostatic pressure at the levee base reached 7.357,5 Pa or 7.357,5Kg/m.s^2 (Figure 4a), with generated stress of 37.830 Kg/m.s^2 (Figure 4b), stress 5,18 x 10^{-6} and deformation of 3,83 x 10^{-5} m (Figure 4c- 4d). Shear force reached 5.518,10 N or 5.518,10 Kg m/s^2, and the safety factor for shear was 3,57, maintaining structural stability (Figure 4e).

Overturning moment analysis showed a hydrostatic moment of 3720 Nm and a resisting moment from the levee weight of 2.744,700 Nm or 2.744,700 Kg m/s^2.m, resulting in a safety factor of 4,49 (Figure 4f).

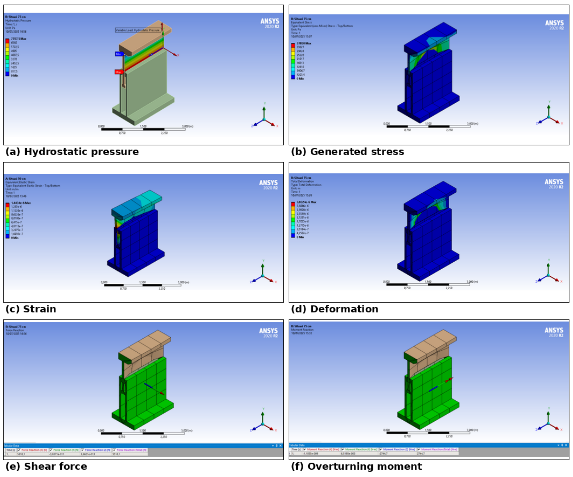

Figure 4. Static structural results for Scenario II (h = 75 cm): (a) hydrostatic pressure, (b) generated stress, (c) strain, (d) deformation, (e) shear force, (f) overturning moment (ANSYS Static Structural)

In Scenario III, representing full high tide (h = 100 cm), hydrostatic pressure reached 9810 Pa or 9810 Kg/m.s^2 (Figure 5a), with stress of 89.662 Kg/m.s^2 (Figure 5b), Stress of 1,24 x 10^{-5} and deformation of 1,24 x 10^{-5} m (Figure 5c – 5d). Shear force was 9.810,00 N or 9.810,00 Kg m/s^2, with a shear safety factor of 2,01, indicating maintained structural integrity (Figure 5e)

The overturning moment due to hydrostatic force was 6.567,600 Nm or 6.567,600 Kg m/s^2.m, while the resisting moment was 16.422,104 Kg m/s^2.m, resulting in a safety factor of 2.50 (Figure 5f).

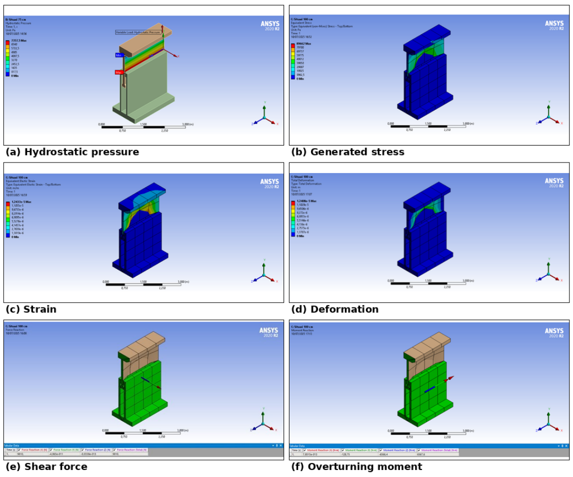

Figure 5a. Static structural results for Scenario III (h = 100 cm): (a) hydrostatic pressure, (b) generated stress, (c) strain, (d) deformation, (e) shear force, (f) overturning moment (ANSYS Static Structural)

Despite differences in stress and deformation across the three scenarios, the floating fiber levee maintained stability under all tested conditions.

Table 2. Summary of ANSYS Modelling Results – Scenarios I, II, and III

Parameter	Unit	Scenario I	Scenario II	Scenario III
Hydrostatic Pressure	$Kg/m^2.s^2$	4905,000	7357,500	9810,000
Maximum Stress (σ)	$Kg/m^2.s^2$	11196,000	37830,000	89662,000
Strain (ε)	–	$1{,}44 \times 10^{-6}$	$5{,}18 \times 10^{-6}$	$1{,}24 \times 10^{-5}$
Deformation (δ)	m	$7{,}63 \times 10^{-6}$	$3{,}83 \times 10^{-5}$	$1{,}24 \times 10^{-5}$
Safety Factor Of Shear	–	8,04	3,57	2,01
Safety Factor Of Moment	–	10,04	4,49	2,50

Despite increasing hydrostatic pressure, shear force, and overturning moment, all safety factors remained within safe limits, both experimentally and in simulation.

3.3. Discussion

This section analyzes the static structural results across Scenarios I–III, comparing manual calculations with ANSYS simulations and assessing their relevance to real-world field conditions and design improvement.

3.3.1. Evaluation of Hydrostatic Pressure and Maximum Stress

Hydrostatic pressure increased from 4905.00 Kg/m^2 (Scenario I) to 9810.00 Kg/m^2 (Scenario III), with identical ANSYS values, since water surface height is the only governing factor—confirming modeling accuracy.

In terms of maximum stress, both approaches showed increasing values with higher water levels. Manual calculations ranged from 11.206,995 $Kg/m^2.s^2$ to 89.655,956 $Kg/m^2.s^2$, while ANSYS results ranged from 11.196 $Kg/m^2.s^2$ to 89.662 $Kg/m^2.s^2$. This close agreement confirms the reliability of the ANSYS modeling for predicting structural stress under varying tidal conditions.

3.3.2. Strain and Deformation Analysis

Strain increased from $1{,}54 \times 10^{-6}$ (Scenario I) to 1.23×10^{-5} (Scenario III) in manual calculations, while ANSYS results showed $1{,}44 \times 10^{-6}$, $5{,}18 \times 10^{-5}$, and $1{,}24 \times 10^{-5}$ respectively.

Deformation followed a similar trend, reaching $1{,}23 \times 10^{-5}$ m (manual) and $1{,}244 \times 10^{-5}$ m (ANSYS) in Scenario III. This rising deformation indicated a functional stress limit in extreme conditions, pointing to the need for material reinforcement.

3.3.3. Stability Against Shear and Overturning

The shear safety factor consistently remained above the critical threshold; however, a progressive reduction was observed across scenarios: 8,04 (Scenario I), 3,57 (Scenario II), and 2,01 (Scenario III). Similarly, the overturning moment safety factor exhibited a marked decline from 10,04 in Scenario I to 2,50 in Scenario III. Although the structure retained its overall stability, the diminishing safety margins underscore the necessity for structural re-engineering of the levee system to enhance its resilience against overturning loads under extreme tidal conditions. Standard engineering practice for hydraulic structures requires a minimum safety factor of 1.5 for both shear and overturning. In Scenario III, SF_shear = 2.01 and SF_moment = 2.50 still exceed this threshold, confirming structural adequacy under full tidal loading. However, the progressive decline in safety factors—approximately 75% reduction in SF_shear from Scenario I to III—indicates that overturning is the governing failure mechanism under extreme conditions. Sensitivity analysis suggests that increasing the base width or adding ballast weight would most effectively improve overturning resistance without significantly increasing the hydrostatic load profile.

3.3.4. Design Implications and Recommendations

The floating fiber levee demonstrated good performance against hydrostatic pressure, shear, deformation, and overturning moment, indicating a fundamentally robust structural system. Further refinement of material properties and structural configuration is nonetheless recommended to ensure long-term reliability under extreme tidal conditions.

ANSYS simulations captured force distribution more realistically than manual calculations, supporting its continued use in future levee design. Compared to the self-closing flood barrier analyzed by Krishnan et al. [19] using ANSYS, which reported deformations in a similar magnitude range under comparable hydraulic loading, the floating fiber levee in this study demonstrated competitive structural performance with the added advantage of dynamic height adjustment. The safety factors obtained in this study are also consistent with the structural performance benchmarks reported for composite marine barriers by Hill and Henderson [22], who documented shear safety factors above 2.0 under design load conditions. These comparisons suggest that the floating fiber composite concept is structurally competitive with established barrier typologies, though further validation under dynamic wave loading remains necessary.

3.3.5. Limitations and Future Research

Across all three tidal scenarios ($h = 50$, 75, and 100 cm), shear and overturning safety factors remained above the minimum engineering threshold, with the lowest values ($SF\_shear = 2.01$; $SF\_moment = 2.50$) at full high tide, identifying overturning as the governing failure mode under extreme loading. ANSYS results showed only minor deviation from manual calculations, confirming the numerical approach's reliability for this class of hydraulic structure. The primary limitation of this study is its prototype-scale scope: scale-up behavior, dynamic wave loading, and long-term material fatigue under marine exposure remain unvalidated. Future research should pursue field-scale prototype testing and base-geometry optimization to further enhance overturning resistance.

4. **Conclusion**

This study confirmed that the floating fiber levee model, evaluated through manual calculations and ANSYS simulation under three tidal scenarios, remained structurally stable, with the narrowest safety margins occurring at full high tide (Scenario III). The declining overturning safety factor at peak tidal load points to base-geometry optimization as a design priority, while the rise in stress and deformation at high tide indicates a need for material reinforcement. These findings support the prototype-scale feasibility of the floating fiber levee concept and provide a foundation for further development toward field-scale, wave-validated implementation.

Declaration of AI and AI assisted technologies in the writing process

The authors declare that no artificial intelligence (AI) or AI-assisted technologies were used in preparing, writing, or editing this manuscript.

Declaration of Competing Interest

The authors declare that they have no known competing financial interests or personal relationships that could have appeared to influence the work reported in this paper.

Acknowledgements
The authors gratefully acknowledge the Laboratory of Civil Engineering, Faculty of Engineering, Sultan Agung Islamic University, and the academic contributions of Wiralodra University and Sekolah Tinggi Teknologi Cirebon.

References

[1] Y. Jiang, W. Finnegan, F. Wallace, M. Flanagan, T. Flanagan, and J. Goggins, “Structural analysis of a fibre-reinforced composite blade for a 1 MW tidal turbine rotor under degradation of seawater,” *Journal of Ocean Engineering and Marine Energy*, vol. 9, no. 3, pp. 477–494, 2023. doi: https://doi.org/10.1007/s40722-023-00279-w

[2] Z. Li, D. Chen, X. Feng, and J. F. Chen, “Hydroelastic analysis and structural design of a modular floating structure applying ultra-high-performance fiber-reinforced concrete,” *Ocean Engineering*, vol. 277, p. 114266, 2023. doi: https://doi.org/10.1016/j.oceaneng.2023.114266

[3] Y. Tang, X. Chen, G. Huang, M. Chen, K. Zhang, Y. Jiang, et al., "Dynamic analysis of multi-module floating photovoltaic platforms with composite mooring system by considering tidal variation and platform configuration," *Ocean Engineering*, vol. 312, p. 119243, 2024, doi: https://doi.org/10.1016/j.oceaneng.2024.119243.

[4] W. Utami, C. Sugiyanto, and N. Rahardjo, “Mangrove area degradation and management strategies in Indonesia: A review,” *J. Degrad. Min. Lands Manag.*, vol. 11, no. 3, pp. 6037–6047, 2024, doi: https://doi.org/10.15243/jdmlm.2024.113.6037.

[5] R. T. Vinata, M. T. Kumala, and P. J. Setyowati, “Blue Carbon Ecosystems for Climate Resilience in Indonesia: A Study of Adaptation Strategy,” *Environmental Policy and Law*, vol. 54, no. 1, pp. 43–51, 2024, doi: https://doi.org/10.3233/EPL-230049.

[6] J. Riffat, S. R. Samaei, and M. A. Ghahfarokhi, “AI-Based Optimization and Hydrodynamic Performance of Floating Pontoon Breakwaters through Experimental and Numerical Modeling,” *Global Decarbonisation*, vol. 1, no. 1, pp. 1–26, 2025. doi: https://doi.org/10.17184/eac.9847

[7] N. V. Golovastikov, N. L. Kazanskiy, and S. N. Khonina, “Optical fiber-based structural health monitoring: advancements, applications, and integration with artificial intelligence for civil and urban infrastructure,” in *Photonics*, vol. 12, no. 6, p. 615, Jun. 2025. doi: https://doi.org/10.3390/photonics12060615

[8] H. Gonabadi, A. Oila, A. Yadav, and S. Bull, “Structural performance of composite tidal turbine blades,” *Composite Structures*, vol. 278, p. 114679, 2021. doi: https://doi.org/10.1016/j.compstruct.2021.114679

[9] A. Serra-Llobet *et al.*, “Restoring rivers and floodplains for habitat and flood risk reduction,” *Frontiers in Environmental Science*, vol. 9, 2022, doi: https://doi.org/10.3389/fenvs.2021.778568.

[10] A. J. Catalano and D. M. Hall, "Reviewing the levee effect: From theory to practice," *Journal of Flood Risk Management*, vol. 19, no. 2, p. e70211, 2026, doi: https://doi.org/10.1111/jfr3.70211.

[11] T. Le Xuan, et al, "Evaluation of coastal protection strategies and proposing multiple lines of defense under climate change in the Mekong Delta for sustainable shoreline protection," *Ocean & Coastal Management*, vol. 228, p. 106301, 2022, doi: https://doi.org/10.1016/j.ocecoaman.2022.106301

[12] E. Amini, R. Marsooli, and B. M. Ayyub, “Characterizing vegetation effects on wave mitigation,” *Environmental Research Communications*, vol. 7, no. 3, p. 035014, 2025, doi: https://doi.org/10.1088/2515-7620/adbc4d.

[13] N. Kaur, M. Mushtaq, and S. Z. Khurshaid, “Comparison of biomechanical differences by FEM,” *International Journal of Health Sciences*, pp. 4127–4146, 2022, doi: https://doi.org/10.53730/ijhs.v6ns9.13620.

[14] M. Nasim and S. Setunge, “A pioneering integration of structural health assessments and dynamic analyses: Bridge pier responses to the impact of floating objects during extreme floods,” *J. Mar. Sci. Eng.*, vol. 12, no. 4, Art. no. 526, 2024, doi: https://doi.org/10.3390/jmse12040526.

[15] C. Y. Zhang and T. Oki, “Water pricing reform for sustainable water resources management in China’s agricultural sector,” *Agricultural Water Management*, vol. 275, p. 108045, 2023, doi: https://doi.org/10.1016/j.agwat.2022.108045.
[16] J. Wang, Y. Liu, and H. Zhang, “Hydrodynamic performance of floating breakwaters under irregular wave conditions,” *Ocean Engineering*, vol. 217, p. 107957, 2020, doi: https://doi.org/10.1016/j.oceaneng.2020.107957.
[17] J. K. Janga, K. R. Reddy, and J. Schulenberg, “Climate change impacts on safety of levees: A review,” in *Geotechnical Engineering Challenges to Meet Current and Emerging Needs of Society*. Boca Raton, FL, USA: CRC Press, 2024, pp. 1669–1674, doi: https://doi.org/10.1201/9781003431749-310.
[18] C. Jiang, Q. Li, P. Hu, G. Zhang, S. Jiang, and O. el Moctar, “Experimental analysis of wave–structure interaction for very large modular floating structures,” *Ocean Engineering*, vol. 315, Art. no. 119763, 2025, doi: https://doi.org/10.1016/j.oceaneng.2024.119763.
[19] L. Krishnan *et al.*, “Analytical study on self closing flood barrier using ANSYS,” *IJERT*, vol. 3, no. 16, pp. 1–4, 2015. doi: https://doi.org/10.17577/IJERTCONV3IS16005
[20] A. Sivasuriyan, et al, "Advanced sensing and digital monitoring technologies for structural health assessment of civil infrastructure," *Buildings*, vol. 16, no. 3, p. 656, 2026, doi: https://doi.org/10.3390/buildings16030656.
[21] J. Muñoz-Caballero, D. Vergara, P. Fernández-Arias, and Á. Antón-Sancho, "Design of a smart barrier to internal flooding," *Inventions*, vol. 7, no. 4, p. 88, 2022, doi: https://doi.org/10.3390/inventions7040088.
[22] K. Hill and G. Henderson, "Pond urbanism: Floating urban districts on shallow coastal groundwater," in *WCFS2020: Proceedings of the Second World Conference on Floating Solutions, Rotterdam*, Singapore: Springer Singapore, 2021, pp. 23–42, doi: https://doi.org/10.1007/978-981-16-2256-4_2.
[23] H. Fatehi, D. E. Ong, J. Yu, and I. Chang, "Biopolymers as green binders for soil improvement in geotechnical applications: A review," *Geosciences*, vol. 11, no. 7, p. 291, 2021, doi: https://doi.org/10.3390/geosciences11070291.
[24] S. Cola, et al, "An optical fiber-based monitoring system to study the seepage flow below the landside toe of a river levee," *Journal of Civil Structural Health Monitoring*, vol. 11, no. 3, pp. 691–705, 2021, doi: https://doi.org/10.1007/s13349-021-00475-y.
[25] H. G. Schlesier, H. von Häfen, and N. Goseberg, "Physical modelling of tsunami barrier and debris interaction," *Journal of Coastal and Hydraulic Structures*, vol. 1, 2021, doi: https://doi.org/10.48438/jchs.2021.0003.